Solar Occultation with SPICAM/UV onboard Mars Express: Retrieving Aerosol and Ozone Profiles

Constantino Listowski, Anni Määttänen, Franck Montmessin, Franck Lefèvre, Jean-Loup Bertaux

SOLAR OCCULTATION WITH SPICAM/UV ON BOARD MARS EXPRESS: RETRIEVING AEROSOL AND OZONE PROFILES.

C. Listowski , *Laboratoire ATmosphères, Milieux, Observations Spatiales (LATMOS), Université Versailles St Quentin (UVSQ), Guyancourt, France (constantino.listowski@latmos.ipsl.fr),* **A. Määttänen**, *LATMOS, UVSQ, Guyancourt, France,* **F. Montmessin**, *LATMOS, UVSQ, Guyancourt, France,* **F. Lefèvre**, *LATMOS, Université Pierre et Marie Curie, Paris, France*, **J.-L. Bertaux**, *LATMOS, UVSQ, Guyancourt, France*

Introduction:

We present the first results of solar occultation performed with the UV channel of SPICAM, on board Mars Express (spectral range of 120-320 nm and resolution of 0.51 nm (Bertaux et al. 2006)). We have analyzed observations from the 21st of April 2004 to 21st of August 2008. In Martian Years, this corresponds to MY27&28, and the beginning of MY29. This dataset of 2.25 Martian years allows interannual and seasonal comparisons of the detected species: ozone (column density and local density) and aerosols (slant opacity, extinction coefficient and effective radius).

Occultation is a powerful technique for the observation of planetary atmospheres because it is self-calibrated, requiring no radiometric registration and being nearly insensitive to instrument aging: at every observation, a reference spectrum of the source is collected to which spectra observed through the atmosphere are compared.

Stellar occultation in UV with SPICAM have already been presented in Quémerais et al. (2006), Montmessin et al. (2006b), Lebonnois et al. (2006), and Forget et al. (2009). These studies present results on CO2, ozone, and aerosols that can be directly used to constrain climate models.

The Martian climate is in great part controlled by the presence and the radiative effect of suspended particles; i.e. mineral dust aerosols and icy condensates. The near-surface winds lift dust from the surface in particular during storms and/or through small-scale vertical phenomena such as dust devils. Dust storms occur mostly when Mars is at perihelion between Ls=220 and Ls=300 (Smith, 2004), corresponding to southern spring/summer. These storms may have a global extent or be regional (Cantor et al., 2001).

SPICAM nadir observations were used to map ozone column densities during more than one Martian Year resulting in the first complete climatology of O3 with a good temporal and spatial resolution (Perrier et al. 2006). SPICAM stellar occultations were used to derive O3 vertical profiles (Lebonnois et al. 2006) that revealed the existence of two ozone layers, a superficial one below 30 km, and another, seasonally and spatially highly variable one, located at 30-60 km. In this work, SPICAM solar occultations are used to complement the existing datasets on the Martian ozone. A parallel work on SPICAM IR solar occultation measurements of water vapor profiles (Maltagliati et al. 2009, 2010) will help to constrain the GCM dynamics and chemistry through a comparison of the well-understood ozone-water vapor anticorrelation (Lefèvre et al. 2004).

Methods:

The CCD has 288 lines, so that theoretically 288 spectra may be resolved. However, only 5 spectra (summation over several CCD lines) are transmitted per second because of telemetry constraints. Thus, the CCD effectively consists of 5 bands (the regions that are summed up) so that a whole set of observation contains 5 tempo-spectra. Each of the 5 bands resolves the vertical profile with a 1 km resolution resulting from the 1 Hz frequency of monitoring the Sun signal. Merging the observed profiles of the 5 bands increases the resolution to 0.2 km on average.

The data processing leading to vertical profiles of aerosols, O3 and CO2 involves three steps (see Quémerais et al., 2006, Montmessin et al., 2006b):

- Determination of atmospheric transmission;
- Spectral inversion leading to column densities and slant opacities;
- Vertical inversion leading to local atmospheric properties (e.g. densities and extinction coefficients).

Figure 1 shows an example of transmission spectra with a color scale related to the altitude of the LOS. The strong ozone absorption (Hartley band) appears around 250nm. The aerosols affect the entire spectrum (slope of the spectra)

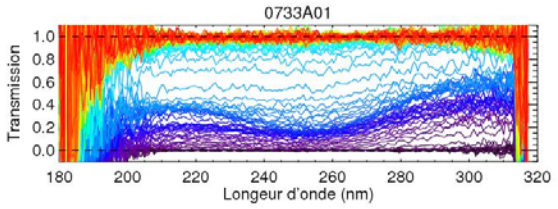

Figure 1: Example of transmission spectra at different altitudes (blue: low altitudes; red: highest altitudes). The transmission is plotted versus the wavelength. The signal is very noisy below 200 nm because of low emission of the sun shortward of 200nm.

Resulting transmission spectra can then be fitted with the simple Beer-Lambert law, allowing the retrieval of absolute quantities (local density or extinction coefficient) from relative (spectral ratio) measurements. The spectral behavior of aerosols is modeled by the α-model (e.g. O'Neill and Royer, 1993) The parameter α gives access to, via Mie theory, the effective radius of particles.

While CO2 can be easily deduced from the occultation of bright UV stars, the Sun is a poor emitter below 200nm and the CO2 retrieval yields very large uncertainties. Thus we use EMCD (European Mars Climate Database v.4.3, Millour et al., 2008) profiles that offer a smoother and more realistic estimation than given by our retrieval, and thereby reduce potential biases affecting the other quantities retrieved.

The vertical inversion process allows to find n(z) and $k_{ext}(z)$, respectively the local density and the extinction coefficient, at an altitude z along the local vertical passing by the MNP, using an onion peeling method which models the atmosphere in discrete concentric layers in which n(z) and kext(z) are constant, varying only from a layer to the next one.

We define here the general name "orbits X000" all the occultations performed during orbits with number $X*1000 \leq N \leq X*1000+1000$. In each group of orbits, the occultations are performed continuously within a period so that $\Delta Ls \leq 70°$.

Results for aerosols:

Among the 720 occultations 450 profiles were analyzed. All the orbits #3000 were rejected because of anomalous behavior: the transmissions computed displayed spurious oscillations. Some other profiles were not considered because of CCD intensifier anomalies.

The hazetop In order to investigate the seasonal and interannual behavior of the dust we define here two cases of aerosol vertical distribution based on observed profiles: 1) The well-mixed layer of dust that starts at the surface extending up to a certain altitude, 2) The detached layers that form above this well-mixed "haze".

Thus a first approach is to undertake the mapping of the depth of the persistent dust haze that is continuously observed in the lowest atmosphere. Jaquin et al. (1986) and more recently Montmessin et al. (2006b) have presented the seasonal variations of this aerosol layer. We define hazetop as the altitude where the opacity of aerosols decreases from its surface value to $\tau aer = 1$ (see Fig. 4): any detached layer above this level is ignored and analyzed separately.

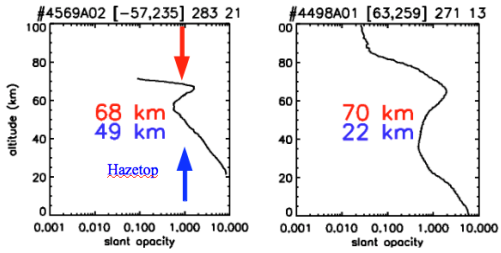

Figure 2: Two examples of slant opacity profiles with a detached layer having a slant opacity greater than 1. The hazetop is shown by the blue arrow, and the red arrow shows the detached haze.

In our study the spatial coverage (in one year) is not as high as in Montmessin et al. (2006b). However, combining the 2.25 Martian Years of observations (MY27-29), we do observe a seasonal signature of the hazetop.

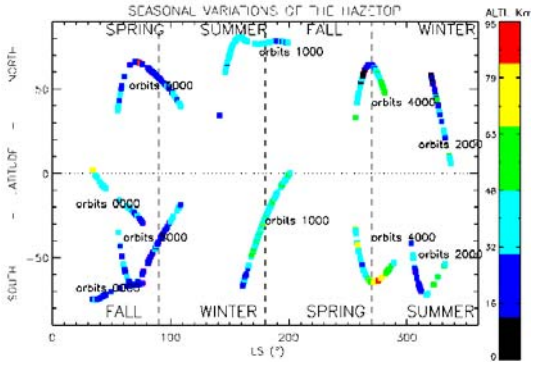

Figure 3: Seasonal variation of the hazetop. We observe higher hazetop values in the warmer regions and seasons, i.e., toward the equator and during southern spring and summer (180°≤ LS ≤ 360°)

Our observations of orbits #0000 (MY 27), and orbits #5000 (MY 29), overlap in the southern hemisphere near 65°S, and display roughly the same average hazetop values of 22-23 km. Thus we can state that the altitude of the hazetop in southern fall is in general around 20-30 km.

Dust storm Another interesting interannual variation in this dataset is the much higher hazetops observed during and after the southern spring equinox in MY 28 (orbits #4000) than those of the southern summer of MY27 (orbits #2000). Both sets of orbits are located in the [70◦S, 50◦S] latitude band and are close in Ls. On average, the hazetop in this season of the MY28 is more than 90% higher than the MY27 one observed only slightly later in the season. The most likely reason is the global dust storm observed at this season during MY28 (also observed with THEMIS: Smith, 2009).

Detached layers In several profiles, clear layers of high opacity at high altitudes have been observed: we have analyzed such layers with statistics performed on the different Martian years of observations. A detached layer may consist of ice condensates or may be a simple dust plume. However, in occultation mode we cannot distinguish between these cases.

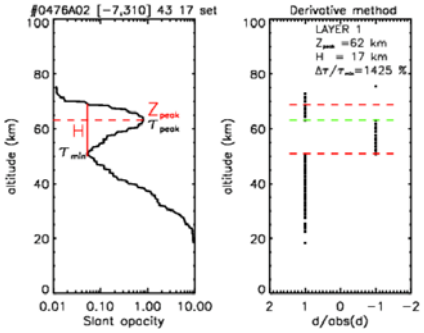

Figure 4: a detection of a layer at Lat=-7°, Long=310°, Ls=43, Lt=17h, during sunset.

We systematically looked for the most clearly defined atmospheric structures. Figure 6 shows an example of detection of a layer (using change of sign in the derivative of the profile $\tau(z)$). About 36 % of

the profiles contain at least one clearly identifiable detached layer. Table 1 summarizes the properties of the detected layers. The maximum layer altitude is observed during the dust storm (90 km) and the maximum vertical extent of a layer is 41 km, during southern summer.

Occultations	Z_{peak} (km)			H (km)			$\Delta\tau/\tau_{min}$ (%)		
	min	max	mean	min	max	mean	min	max	mean
orbits0000	23.7	69.6	41.1	3.0	29.6	7.7	6.1	1368.6	139.9
orbits1000	18.4	78.1	55.0	2.8	29.6	13.2	3.5	374.5	51.8
orbits2000	47.8	80.9	55.8	7.7	40.6	23.4	9.3	156.9	71.0
orbits4000	60.6	90.4	71.4	5.0	34.9	14.5	26.1	558.7	178.3
orbits5000	22.2	77.8	36.7	3.1	28.3	13.7	6.7	620.8	71.3

Table 1: Mean characteristics of the observed detached layers: the peak layer altitude Zpeak, the vertical extension of the layer H, and the increase of the opacity within the layer in percentage $\Delta\tau/\tau$min.

The average Zpeak in orbits #4000 (global dust storm) is 71 km, at least 15 km higher on average compared to the orbits 2000 closest in latitude and season.

The lowest detached layers (see Fig. 7) were found in the northern set of the orbits 1000, which were monitored above polar regions during late summer with Zpeak reaching 18-22 km. Although the layers observed with SPICAM are not in the PBL, we interestingly find the lowest layers in the same latitudes and during the same part of the northern summer where Whiteway et al. (2009) detected the formation of PBL clouds.

Radius: haze and detached layers The vertical distribution of aerosols is a result of a complex interplay between gravitational settling, vertical transport and interactions between condensates and dust aerosols. In general, because of gravitational settling, larger particles are found at lower altitudes (Fig.8).

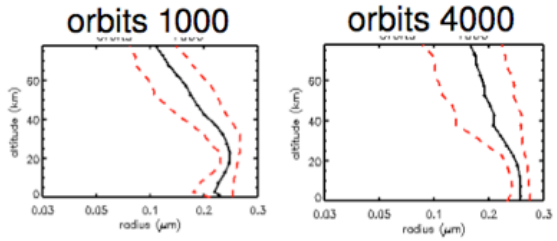

Figure 5: mean radius (µm) VS altitude (m) for orbits 1000 and orbits 4000. The red dashed lines show the variance of the averaged profiles

Nevertheless, large particles may be observed at high altitudes in the case of cloud formation, when an ice shell forms a dust grain. Some layers show radii 150% larger than the values observed just below the layer.

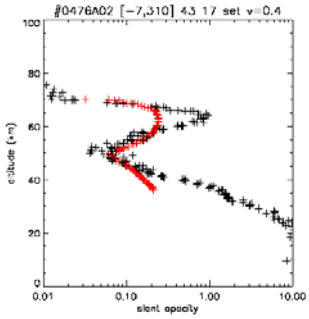

Figure 6: Example of an increase in radius (in µm, in red) in a detached layer (slant opacity in black).

Figure 9 shows a profile where the radius increases from 60nm below the layer up to of 290nm inside the layer. Conversely to the near-surface haze that shows a decreasing trend of radius with altitude, the radii in the detached layers do not show a similar trend (Fig. 10).

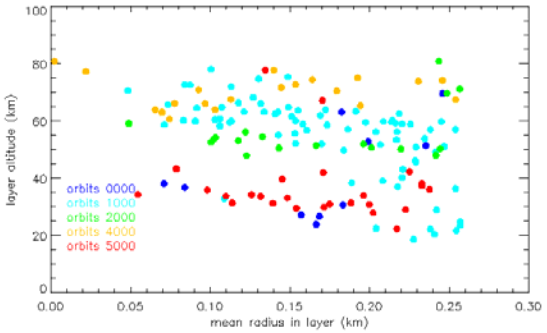

Figure 7: layer altitude (km) VS mean radius in the detached layers (µm). The different colors are related to the different sets of orbits.

Considering only orbits 1000 (light blue on Fig. 10) the bigger mean radii are observed in the lowest layers at high northern latitudes.

First results for ozone:

Ozone layer Ozone profiles were derived and compared with the modeled climatology of O3 (Lefèvre et al. 2004). Figure 11 shows three examples of Slant column of O3 (molecule.cm-2). We observe the nocturnal ozone layer at an altitude around 30-60 km, observed by Lebonnois et al. (2006) and predicted by models. Since we observe the atmosphere at the terminator (during sunrise or sunset) we can conclude that the nocturnal ozone layer is already (still) present during sunset (sunrise).

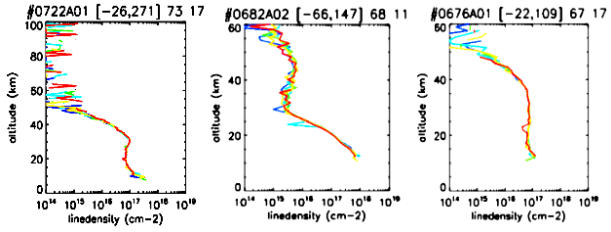

Figure 8: Three Slant column of O3 (molecule.cm-2). Different colors are related to the different bands of a single observation. Two profiles with an ozone layer (~30 km at sunset and ~40 km at sunrise) are shown. Note the different altitude ranges.

Comparison with the LMD-GCM Comparisons were done with the profiles obtained from the LMD-

GCM (Lefèvre et al. 2004), and the first results show good agreement (Figure 12).

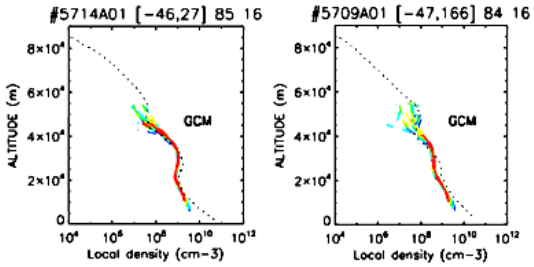

Figure 9: Two comparisons of local density (cm-3) profiles of the LMD-GCM (dotted line) with our observations.

Conclusion and perspectives:

We present a large dataset of 2.25 Martian Years (MY27-29) of SPICAM/UV solar occultations. We derived aerosol and ozone vertical profiles that can extend to very low altitudes (~10 km). We investigate the aerosol vertical distribution and its seasonal variations through monitoring the haze adjacent to the surface and the detached layers that may form above it. The multiannual dataset allowed us to monitor the dust seasonal cycle. We also observed the consequences of the MY28 dust storm (higher haze-top and higher detached layers) in the southern hemisphere. The lowest layers are observed at high northern latitudes, with large particles of a mean radius between 200 and 300 nm. The ozone profiles confirm the previously observed nocturnal layers (Lebonnois et al. 2006) at sunrise and sunset during the same period. First comparisons with ozone profiles from the LMD-GCM show good agreement. Further comparisons with model profiles will be done for ozone and the water vapor profiles of SPICAM/IR (Maltagliati et al. 2009, 2010): this will allow to better constrain the water-ozone anticorrelation in the LMD-GCM (Lefèvre et al. 2004). Since the solar occultation mode observes at sunrise or sunset at a given location, comparisons of ozone profiles at morning and evening terminator (where atmospheric chemistry might drastically change) would be interesting.

References:

Bertaux, J., Korablev, O., Perrier, S., Qu´emerais, E., Montmessin, F., Leblanc, F., Lebonnois, S., Rannou, P., Lef´evre, F., Forget, F., Fedorova, A., Dimarellis, E., Reberac, A., Fonteyn, D., Chaufray, J. Y., Guibert, S., 2006. SPICAM on Mars Express: Observing modes and overview of UV spectrometer data and scientific results. Journal of Geophysical Research (Planets) 111 (E10), 10–+

Cantor, B. A., James, P. B., Caplinger, M., Wolff, M. J., 2001. Martian dust storms: 1999 Mars Orbiter Camera observations. J. Geophys. Res. 106 (E10), 23653–23687.

Forget, F., Montmessin, F., Bertaux, J.-L., Gonz´alez-Galindo, F., Lebonnois, S., Qu´emerais, E., Reberac, A., Dimarellis, E., L´opez-Valverde, M. A., 2009. The density and temperatures of the upper martian atmosphere measured by stellar occultations with Mars Express SPICAM. J. Geophys. Res. 114, E01004, doi:10.1029/2008JE003086.

Jaquin, F., Gierasch, P., Kahn, R., Dec. 1986. The vertical structure of limb hazes in the Martian atmosphere. Icarus 68, 442–461.

Lebonnois S., E. Quémerais, F. Montmessin, F. Lefèvre, S. Perrier, J.-L. Bertaux, and F. Forget, 2006: Vertical distribution of ozone on mars as measured by SPICAM/Mars Express using stellar occultations. J. Geophys. Res. 111, E09S05.

Lefèvre, F., S. Lebonnois, F. Montmessin, and F. Forget (2004), Three-dimensional modeling of ozone on Mars, J. Geophys. Res., 109, E07004, doi:10.1029/2004JE002268.

Maltagliati, L., Fedorova, A., Montmessin, F., Bertaux, J., Korablev, O., Reberac, A. (2009), Vertical Profiles Of Water Vapor In Mars' Atmosphere By Spicam/mex Solar Occultations, 41st annual meeting of the Division for Planetary Sciences of the American Astronomical Society, Pasadena, California, 2009, abstract number 44.06

Maltagliati, L., Fedorova, A., Montmessin, F., Bertaux, J., Korablev, O., Reberac, A. (2010), Discoveries on the vertical distribution of water vapor in Mars' atmosphere as observed by the SPICAM-IR spectrometer, AGU Fall Meeting, 13-17 December 2010, San Francisco (US), P51E-11

Millour, E., Forget, F., Gonza´lez-Galindo, F., Spiga, A., Lebonnois, S., Montabone, L., Lewis, S. R., Read, P. L., L´opez-Valverde, M. A., Gilli,
21G., Lef´evre, F., Montmessin, F., Desjean, M., Huot, J., The McD/Gcm Development Team, 2008. The Latest (Version 4.3) Mars Climate Database. LPI Contributions 1447, 9029–+.

Montmessin, F., Quémerais, E., Bertaux, J.-L., Korablev, O., Rannou, P., Lebonnois, S., 2006b. Stellar occultations at UV wavelengths by the SPI- CAM instrument: Retrieval and analysis of Martian haze profiles. J. Geophys. Res. 111, E09S09, doi:10.1029/2005JE002662.

O'Neill, N., Royer, A., Mar. 1993. Extraction of bimodal aerosol size distribution radii from spectral and angular slope (Angstrom) coefficients. Applied Optics 32, 1642–1645.

Perrier, S., J.-L. Bertaux, F. Lefèvre, S. Lebonnois, O. Korablev, A. Fedorova, and F. Montmessin, 2006: Global distribution of total ozone on Mars from SPICAM/MEX UV measurements. J. Geophys. Res. 111, E09S06.

Quémerais, E., Bertaux, J., Korablev, O., Dimarellis, E., Cot, C., Sandel, B. R., Fussen, D., Sep. 2006. Stellar occultations observed by SPICAM on Mars Express. J. Geophys. Res. 111, 9–+.

Smith, M. D., 2004. Interannual variability in TES atmospheric observations in Mars during 1999–2003. Icarus 167,148–165.

Smith, M. D., Aug. 2009. THEMIS observations of Mars aerosol optical depth from 2002-2008. Icarus 202, 444–452.

Whiteway, J., Komguem, L., Dickinson, C., Cook, C., Illnicki, M., Popovici, V., Seabrook, J., Daly, M., Carswell, A., Taylor, P., Davy, R., Pathak, J., Lange, C., Fisher, D., Hipkin, V., Tamppari, L., Lemmon, M., Renno, N., Gunnlaugsson, H., Drube, L., Holstein-Rathlou, C., Smith, P., Dec. 2008. Observations of Dust, Ice Water Clouds, and Precipitation in the Atmosphere of Mars. AGU Fall Meeting Abstracts, A9+.